Research Article
Experimental and Translational Hepatology

JOURNAL
OF HEPATOLOGY

EMC10 modulates hepatic ER stress and steatosis in an isoform-specific manner

Authors

Kuangyang Chen, Yahao Wang, Jia Yang, …, Arne Dietrich, Matthias Blüher, Xuanchun Wang

Correspondence

wangxch@fudan.edu.cn (X. Wang).

Graphical abstract

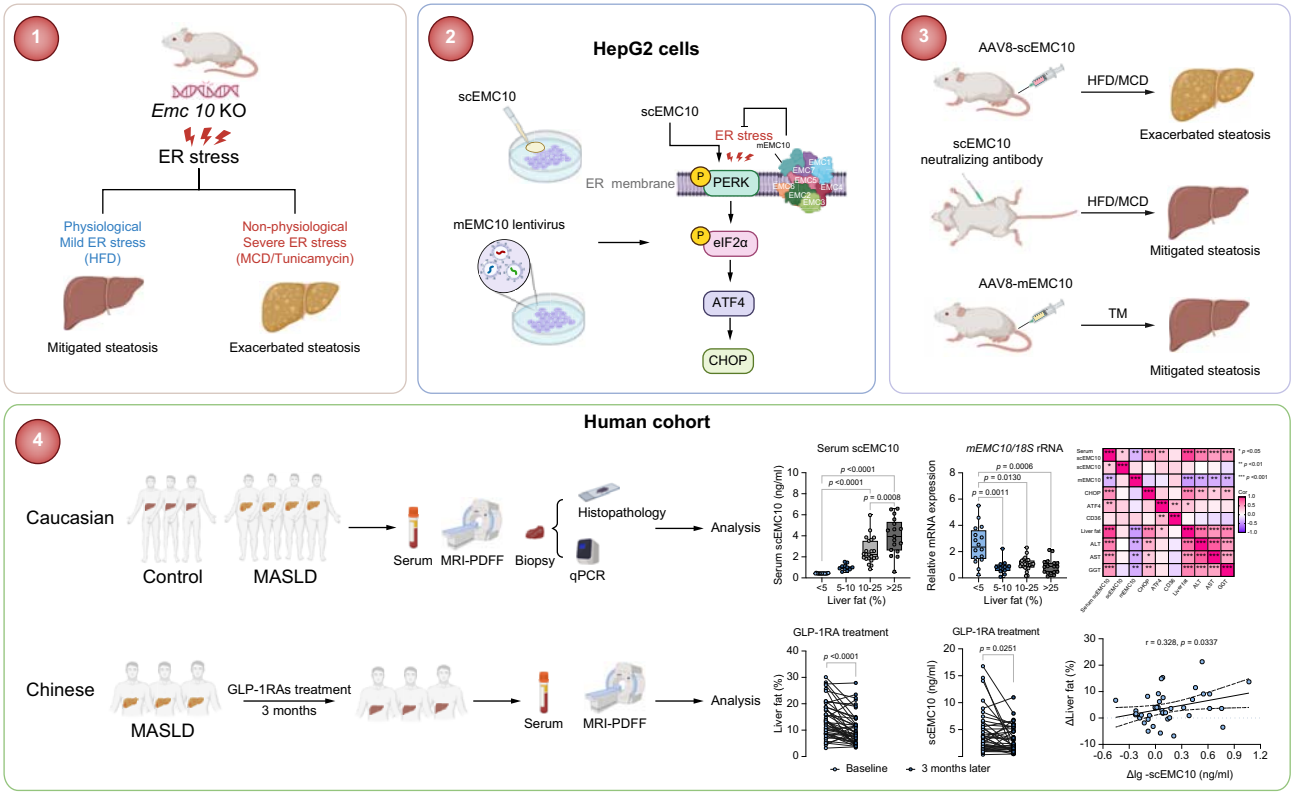

Highlights

- scEMC10 promotes, while mEMC10 suppresses, hepatic ER stress and steatosis in mice.
- scEMC10-neutralizing antibody ameliorates hepatosteatosis in mice with fatty liver.
- Serum scEMC10 positively, while hepatic mEMC10 negatively, correlates with MASLD in humans.
- GLP-1RAs decrease both serum scEMC10 and liver fat content in participants with MASLD.

Impact and implications

We have shown the role of EMC10 in the regulation of energy homeostasis and obesity. In this study, we determine the distinct roles of the two isoforms of EMC10 in the regulation of hepatic endoplasmic reticulum stress and steatosis in mice, and report on the associations of the different EMC10 isoforms with metabolic dysfunction-associated steatotic liver disease in humans. Our findings delineate a novel regulatory axis for hepatosteatosis and identify EMC10 as a modulator of the PERK-eIF2α-ATF4 signaling cascade that may be of broad physiological significance. Moreover, our pre-clinical and clinical studies provide evidence of the therapeutic potential of targeting scEMC10 in MASLD.

https://doi.org/10.1016/j.jhep.2024.03.047
 J. Hepatol. 2024, 81, 479–491

Research Article
Experimental and Translational Hepatology

JOURNAL
OF HEPATOLOGY

EMC10 modulates hepatic ER stress and steatosis in an isoform-specific manner

Kuangyang Chen[1,7,†], **Yahao Wang**[1,†], **Jia Yang**[1,†], Nora Klöting[2,3], Chuanfeng Liu[4], Jiarong Dai[1], Shuoshuo Jin[1], Lijiao Chen[1], Shan Liu[1], Yuzhao Liu[4], Yongzhuo Yu[4], Xiaoxia Liu[1], Qing Miao[1], Chong Wee Liew[5], Yangang Wang[4], Arne Dietrich[6], Matthias Blüher[2,3], Xuanchun Wang[1,*]

Journal of Hepatology **2024**. vol. 81 | 479–491

Background & Aims: Endoplasmic reticulum (ER) membrane protein complex subunit 10 (EMC10) has been implicated in obesity. Here we investigated the roles of the two isoforms of EMC10, including a secreted isoform (scEMC10) and an ER membrane-bound isoform (mEMC10), in metabolic dysfunction-associated steatotic liver disease (MASLD).
Methods: Manifold steatotic mouse models and HepG2 cells were employed to investigate the role of EMC10 in the regulation of hepatic PERK-eIF2α-ATF4 signaling and hepatosteatosis. The therapeutic effect of scEMC10-neutralizing antibody on mouse hepatosteatosis was explored. Associations of MASLD with serum scEMC10 and hepatic mEMC10 were determined in two cohorts of participants with MASLD.
Results: scEMC10 promoted, while mEMC10 suppressed, the activation of hepatic PERK-eIF2α-ATF4 signaling. *Emc10* gene knockout exacerbated, while hepatic overexpression of mEMC10 ameliorated, hepatic ER stress and steatosis in mice challenged with either a methionine- and choline-deficient diet or tunicamycin, highlighting a direct, suppressive role of mEMC10 in MASLD via modulation of hepatic ER stress. Overexpression of scEMC10 promoted, whereas neutralization of circulating scEMC10 prevented, hepatosteatosis in mice with fatty liver, suggesting a role of scEMC10 in MASLD development. Clinically, serum scEMC10 was increased, while hepatic mEMC10 was decreased, in participants with MASLD. Correlative analysis indicated that serum scEMC10 positively, whereas hepatic mEMC10 negatively, correlated with liver fat content and serum ALT, AST, and GGT.
Conclusions: These findings demonstrate a novel isoform-specific role for EMC10 in the pathogenesis of MASLD and identify the secreted isoform as a tractable therapeutic target for MASLD via antibody-based neutralization.

Introduction

Endoplasmic reticulum (ER) stress has been implicated in manifold metabolic diseases including metabolic dysfunction-associated steatotic liver disease (MASLD).[1] In the context of ER stress, an adaptive mechanism known as the unfolded protein response (UPR) is activated and exerts protective effects on the hepatocyte if operating moderately and adequately. However, prolonged or severe UPR leads to the development of hepatosteatosis, the primary stage of MASLD.[2] Steatosis in turn exacerbates ER stress, constituting a vicious cycle between hepatosteatosis and ER stress.[2] The PERK-eIF2α-ATF4 pathway, one arm of the UPR, has been widely implicated in hepatosteatosis. In humans, eIF2α phosphorylation is increased in fatty liver and reduced with the resolution of steatosis achieved by weight loss.[3,4] In mice, heightened hepatic eIF2α phosphorylation has also been observed in fatty liver,[5,6] and sustained dephosphorylation of hepatic eIF2α attenuates high-fat diet (HFD)-induced hepatosteatosis.[7] ATF4 ablation prevents, while its overexpression promotes, hepatosteatosis in mice and zebrafish, respectively.[8–10]

ER membrane protein complex (EMC) has regulatory roles in several cellular processes, including ER stress, aberrant membrane protein trafficking and degradation.[11–13] EMC10, one subunit of EMC, consists of two isoforms in humans and rodents, including a secreted isoform (scEMC10) and an ER membrane-bound isoform (mEMC10).[14] Previously we demonstrated that the two isoforms of EMC10 play distinct roles in male fertility.[15,16] In addition, our recent work revealed that scEMC10 overexpression promoted, while antibody neutralization of circulating scEMC10 or *Emc10* gene knockout (*Emc10* KO), prevented diet-induced obesity, insulin resistance, glucose intolerance, and fatty liver in mice.[17] Clinically, serum scEMC10 was increased in obesity and positively associated with insulin resistance and BMI, whereas it was negatively correlated with resting metabolic rate in humans.[17,18]

In this study, we used multiple mouse models of hepatosteatosis, in combination with cell culture experiments, to

Keywords: secreted EMC10; membrane-bound EMC10; MASLD; hepatosteatosis; ER stress; PERK-eIF2α-ATF4 signaling.
Received 30 January 2024; received in revised form 26 March 2024; accepted 27 March 2024; available online 8 April 2024
* Corresponding author. Address: Department of Endocrinology, Huashan Hospital, 12 Wulumuqi Road (Middle), Shanghai 200040, China; Tel.: 86-21-52888286, fax: 86-21-62495490.
E-mail address: wangxch@fudan.edu.cn (X. Wang).
† Equal contribution
https://doi.org/10.1016/j.jhep.2024.03.047

investigate the roles of the two isoforms of EMC10 in hepatic PERK-eIF2α-ATF4 signaling and steatosis, and determined the associations of the two isoforms with MASLD in humans.

Materials and methods

Animals

To establish mouse models with fatty liver, male mice at 7-8 weeks old were maintained on a HFD (Research Diets, D12492) for 12 or 20 weeks, or a methionine- and choline-deficient (MCD) diet (Research Diets, A02082002BR) for 3 or 6 weeks.

To establish mouse models with acute ER stress, male mice aged 7-8 weeks were injected intraperitoneally with tunicamycin (1 mg per kg body weight) for 24 or 48 hours.

To overexpress different isoforms of EMC10 *in vivo*, adeno-associated virus 8 (AAV8), encoding human scEMC10 (AAV8-scEMC10), or mouse mEMC10 (AAV8-mEMC10), or control virus (AAV8-null) (Hanbio, Shanghai, China) were injected into the tail vein of mice aged 4-5 weeks.

To investigate the role of scEMC10 in the regulation of hepatic PERK-eIF2α signaling *in vivo*, 7-8-week-old male C57BL/6J mice were injected intraperitoneally with recombinant mouse scEMC10 (PZ0104, Phrenzer Biotechnology, Shanghai, China) (6 mg per kg body weight) or vehicle PBS for 30 minutes.

To neutralize circulating scEMC10, male C57BL/6J mice at the age of 7-8 weeks were intraperitoneally injected with mouse monoclonal antibodies against human scEMC10 (PZ0103, Phrenzer Biotechnology, Shanghai, China) (4C2 Ab, 10 mg per kg body weight) or control mouse IgG twice weekly.

All animal studies were conducted with the approval of the Animal Experimentation Ethics Committee of Huashan hospital, Shanghai, China.

Cell culture

HepG2 cells were kindly gifted by Dr. Junli Liu at Shanghai Sixth People's Hospital. Cells were cultivated in DMEM (Bioind, Israel) supplemented with 10% fetal bovine serum (Gibco, Waltham, USA) and 1% streptomycin/penicillin (Gibco, Waltham, USA) at 37 °C and 5% CO2.

Lentivirus packaging and cell transfection

A full-length cDNA encoding human mEMC10 was constructed in the pLEX plasmid by Genomeditech (Shanghai, China). pMD·2G and psPAX2 plasmids as well as 293T cells were kindly gifted by Dr. Daming Gao at Shanghai Institute of Biochemistry and Cell Biology, Chinese Academy of Sciences. Lentivirus was produced in 293T cells by co-transfecting the three plasmids mentioned above. 48 h post transfection, virus-containing supernatant was collected and filtered through 0.45 μm filters. HepG2 cells were transfected with mEMC10-expressing lentivirus in aid of polybrene (40804ES, Yeasen, Shanghai, China) and then selected using 2 μg/ml puromycin (A1113803, Gibco, Waltham, USA).

Human studies

Cohort 1

We investigated *scEMC10, mEMC10, CHOP, CD36, ATF4* mRNA expression in liver tissue samples obtained from 66 extensively characterized Caucasian men (n = 37) and women (n = 29) with a wide range of BMI (22.7-45.6 kg/m^2) who underwent open abdominal surgery (Roux en Y bypass, sleeve gastrectomy, elective cholecystectomy or explorative laparotomy). All study protocols have been approved by the Ethics committee of the University of Leipzig (363-10-13122010 and 017-12-230112). All participants gave written informed consent before taking part in the study.

Cohort 2

A total of 45 participants with MASLD were recruited in the observational study. These participants were treated with GLP-1 receptor agonists (GLP-1RAs), including liraglutide, dulaglutide, exenatide or polyethylene glycol loxenatide for 3 months. This study was approved by the ethics committee of the Affiliated Hospital of Qingdao University (approval number: QYFYWZLL15560) following the principles of the Declaration of Helsinki. All participants gave written informed consent before taking part in the study.

Measurement of scEMC10 in human serum

Serum scEMC10 was measured using a double sandwich ELISA kit (PZ0101, Phrenzer Biotechnology, Shanghai, China) following the manufacturer's instructions.

Gene expression in human liver tissue

Human *scEMC10, mEMC10, CHOP, CD36, ATF4* mRNA expression was measured by quantitative real-time reverse-transcription PCR in a fluorescent temperature cycler using the TaqMan assay, and fluorescence was detected on an ABI PRISM 7000 sequence detector (Applied Biosystems, Darmstadt, Germany).

Statistical analyses

For mouse models and *in vitro* studies, all statistical analyses were carried out using GraphPad Prism 8.4.3. Data were presented as the means ± SEM. Statistical significance was calculated using Student's *t* test for comparison of two groups and one-way ANOVA followed by Tukey's multiple-comparisons test for comparison among multiple groups. $p < 0.05$ was considered statistically significant.

For anthropometric and metabolic characteristics, serum scEMC10 concentration, and human hepatic mRNA levels, all analyses were performed with Statistical Package for Social Sciences version 22.0 (SPSS, Chicago, IL, USA) and figures were graphed with GraphPad Prism 8.4.3 (La Jolla, CA, USA). Normally distributed data were expressed as means ± SD. Data that were not normally distributed, as determined using Kolmogorov-Smirnov test, were expressed as median with interquartile range. Student's paired *t* test or Wilcoxon signed-rank test was used for comparison before and 3 months after GLP-1RA treatment. Pearson's correlation was used to evaluate the correlations among liver fat content, serum scEMC10 levels, hepatic mRNA levels of *scEMC10, mEMC10, CHOP, CD36, ATF4*, and serum alanine aminotransferase (ALT), aspartate aminotransferase (AST), and gamma-glutamyltransferase (GGT). $p < 0.05$ was considered statistically significant.

Details on the materials and methods are provided in the supplementary information and Supplementary CTAT Table.

Results

Ablation of EMC10 ameliorates hepatosteatosis in mice fed a HFD

In our previous study, we demonstrated that ablation of EMC10 decreased hepatic lipid content in HFD-fed mice.[17] To further characterize the role of EMC10 in steatotic liver disease, we conducted a detailed phenotypic assessment of liver health in HFD-fed *Emc10* KO mice. As expected, *Emc10* KO mice were significantly leaner than wild-type (WT) controls in the context of HFD (Fig. S1A). There was no difference in liver index, a ratio of liver mass to body weight, between *Emc10* KO and WT mice, which can be accounted for by the reduced body weights of KO mice (Fig. S1B). Hepatosteatosis, however, was significantly reduced in *Emc10* KO *vs.* WT mice, as evidenced by significantly lower levels of liver fat content (LFC) and plasma lipids and AST (Fig. S1C–F). Steatosis develops as a result of dysregulation of liver lipid metabolism where the rate of fatty acid (FA) accumulation including FA uptake and lipogenesis is greater than that of FA catabolism mainly achieved by FA beta oxidation.[19] Three categories of genes involved in lipid metabolism were investigated in livers from *Emc10* KO and WT mice, including genes related to lipogenesis, FA uptake, and beta oxidation. We observed the mRNA levels of both lipogenic and FA-uptake genes were significantly lower in KO livers than WT ones (Fig. S1G,H), which accounts for the attenuated steatosis in KO mice. Unexpectedly, expression of beta-oxidation genes was also significantly downregulated in KO livers compared with WT ones (Fig. S1I), which is likely a consequence of reduced LFC. Hepatosteatosis is often accompanied by hepatic inflammation and fibrosis.[20] As expected, inflammation was lower in KO compared to WT livers (Fig. S1J). Hepatic fibrosis, however, remained unchanged between KO and WT mice (Fig. S1K). We also observed that some genes involved in ER stress were altered in KO mice, hepatic expression of both *Atf4* and *Chop* significantly decreased, whereas that of *Grp78*, *Xbp1*, and *Atf6*, remained unchanged in KO livers compared with WT controls (Fig. S1L). Taken together, these data indicate that ablation of EMC10 prevents HFD-induced hepatosteatosis.

Ablation of EMC10 exacerbates hepatosteatosis in mice fed a MCD diet

To further explore the impact of EMC10 on hepatosteatosis, we proceeded with another steatotic animal model. A MCD diet is frequently used as a model of steatosis with hepatic inflammation and fibrosis.[21] In contrast to our observations in the context of HFD feeding, MCD diet feeding resulted in marked weight losses in both groups (Fig. 1A). MCD diet-fed *Emc10* KO mice, compared to WT controls, displayed increased liver index and exacerbated hepatosteatosis, as evidenced by greater LFC, NAFLD activity score (NAS), and levels of plasma lipids and ALT (Fig. 1B–G). *Emc10* KO mice exhibited a significant reduction in expression of lipogenic genes in livers compared with WT mice, seemingly inconsistent with the greater degree of steatosis (Fig. 1H). Inhibition of hepatic lipogenesis has been regarded as a negative feedback mechanism in response to excessive LFC caused by the inability to secrete triglycerides in MCD diet-fed mice.[21,22] Therefore, the inhibition of lipogenesis is likely a compensatory response to increased LFC in *Emc10* KO mice. A previous study revealed that the MCD diet increased FA uptake in mouse livers by inducing FA uptake genes, suggesting upregulation of FA uptake as a mechanism underlying MCD diet-induced hepatosteatosis.[21] In this study, we observed greater expression of FA-uptake genes in *Emc10* KO than WT livers (Fig. 1I). The significant reduction in expression of beta-oxidation genes was also congruent with the enhanced steatosis in KO mice compared with WT controls (Fig. 1J). Consistent with exacerbated hepatosteatosis, *Emc10* KO mice displayed increased hepatic inflammation, fibrosis, and ER stress compared with WT animals (Fig. 1K–M).

Extended feeding of a MCD diet further exacerbated body weight loss and hepatosteatosis in both *Emc10* KO and WT mice (Fig. S2). When compared with WT controls, *Emc10* KO mice still displayed greater steatosis, as evidenced by significant increases of liver index and LFC (Fig. S2B–E). Surprisingly, plasma lipids were significantly decreased in KO mice compared with controls (Fig. S2F), probably due to greater mobilization of lipids in KO livers. Extended MCD diet feeding also resulted in greater FA uptake, lesser beta oxidation, and higher levels of inflammation, ER stress and fibrosis in KO livers compared with WT ones, as indicated by gene expression profiles and Sirus Red staining for fibrosis (Fig. S2G–M).

In summary, contrary to the HFD paradigm, MCD diet-fed *Emc10* KO mice develop exacerbated hepatic steatosis, suggesting EMC10 modulates hepatosteatosis in a context-dependent manner.

Ablation of EMC10 exacerbates hepatosteatosis in a mouse model of acute ER stress

The differential effects of EMC10 KO in two different experimental paradigms of mouse hepatosteatosis prompted us to explore the mechanism underlying EMC10-modulated hepatosteatosis. It has been demonstrated that both HFD and MCD diet feeding activate PERK-eIF2α signaling in mouse liver.[5,23] We next employed a mouse model of acute ER stress to investigate whether the PERK-eIF2α pathway is involved in EMC10-regulated hepatosteatosis. Short-term administration of tunicamycin dramatically induces an acute ER stress response and hepatosteatosis caused by impaired FA beta oxidation.[24,25] We observed that tunicamycin administration apparently increased lipid accumulation in WT mouse livers without changes in body weight and liver index (Fig. S3A–C), which we attribute to increased FA uptake and decreased beta oxidation in the livers (Fig. S3D–F). Meanwhile, hepatic PERK-eIF2α signaling was significantly activated by tunicamycin (Fig. S3G). EMC10 ablation significantly increased tunicamycin-induced hepatosteatosis, as evidenced by greater levels of liver index, LFC, and serum ALT and AST in KO mice than WT controls (Fig. 2A–G). *Emc10* KO livers exhibited significantly increased FA uptake, decreased beta oxidation, and heightened fibrosis compared with WT controls (Fig. 2H–K). *Emc10* KO mice, compared to WT ones, also exhibited significant increases in expression of hepatic *Grp78*, *Atf4* and *Chop*, while expression of *Xbp1* and *Atf6* were unchanged, suggesting activation of the PERK-eIF2α arm of the UPR (Fig. 2L). These data, in combination with observations on MCD diet-fed mice, indicate EMC10 ablation failed to cope with ER stress, in turn exacerbating hepatosteatosis via activation of hepatic PERK-eIF2α-ATF4 signaling.

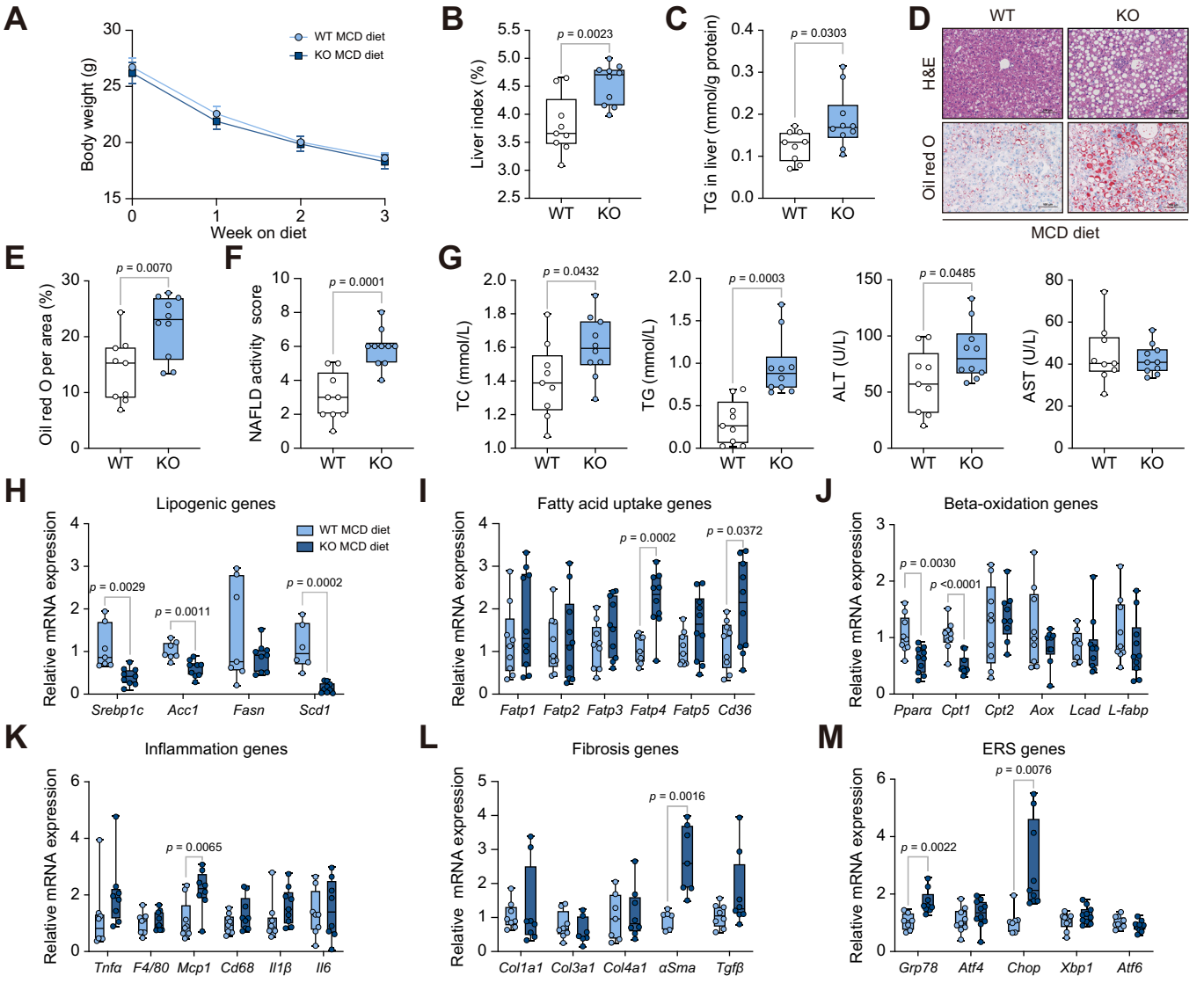

Fig. 1. *Emc10* KO mice develop exacerbated hepatosteatosis under the condition of 3-week MCD diet feeding. WT (n = 9) and *Emc10* KO (n = 10) male mice were fed with a MCD diet for 3 weeks. (A) Body weights. (B) Liver index assessed as a ratio of liver mass to body weight. (C) Liver triglyceride content. (D) Representative images of H&E and Oil red O staining of liver sections. Scale bars, 100 μm. (E) Liver Oil red O staining area. (F) NAFLD activity score. (G) Serum levels of TC, TG, ALT, and AST. (H-M) Relative hepatic expression of genes as indicated, linked to lipogenesis (H), fatty acid uptake (I), beta oxidation (J), inflammation (K), fibrosis (L), and ER stress (M). All data are presented as mean ± SEM. Statistical analyses were performed using Student's *t* test. ALT, alanine aminotransferase; AST, aspartate aminotransferase; ERS, endoplasmic reticulum stress; KO, knockout; MCD, methionine- and choline-deficient; TC, total cholesterol; TG, triglyceride; WT, wild-type. (This figure appears in color on the web.)

EMC10-regulated PERK-eIF2α signaling in mouse liver

To clarify the role of the UPR in EMC10-regulated hepatosteatosis, we determined hepatic activities of the PERK-eIF2α pathway in livers of *Emc10* KO mice *vs.* WT controls. The reason we choose this pathway, but not the other two pathways, *i.e.* IRE1a-XBP1 and ATF6 pathways, is based on the observation that hepatic gene expression of *Atf4* and *Chop*, the key components of PERK-eIF2α signaling, was significantly changed in *Emc10* KO mice, whereas gene expression of both *Xbp1* and *Atf6*, the markers of the other two UPR arms, remained unaffected (Figs 1M, Fig. 2L, and Fig. S1L). We firstly evaluated activity of PERK-eIF2α signaling in livers of mice fed a chow diet. Of note, the signaling was dramatically suppressed in *Emc10* KO mice compared with WT controls, as determined by the levels of both phosphorylated PERK and eIF2α, as well as the abundance of GRP78 and CHOP protein in the livers (Fig. 3A). Steatosis, however, was not different between KO and WT mice in the context of chow diet feeding (Fig. S4). When fed a HFD, *Emc10* KO mice exhibited significantly decreased levels of eIF2α phosphorylation (Fig. 3A) and improved steatosis (Fig. S1) compared with WT mice. However, when challenged with either a MCD diet or tunicamycin, *Emc10* KO mice displayed significantly increased activity of hepatic PERK-eIF2α-ATF4 signaling compared with WT controls (Fig. 3B,C), congruent with their exacerbated hepatosteatosis (Figs 1 and 2). Collectively, these data suggest EMC10 is required for the maintenance of hepatic UPR homeostasis.

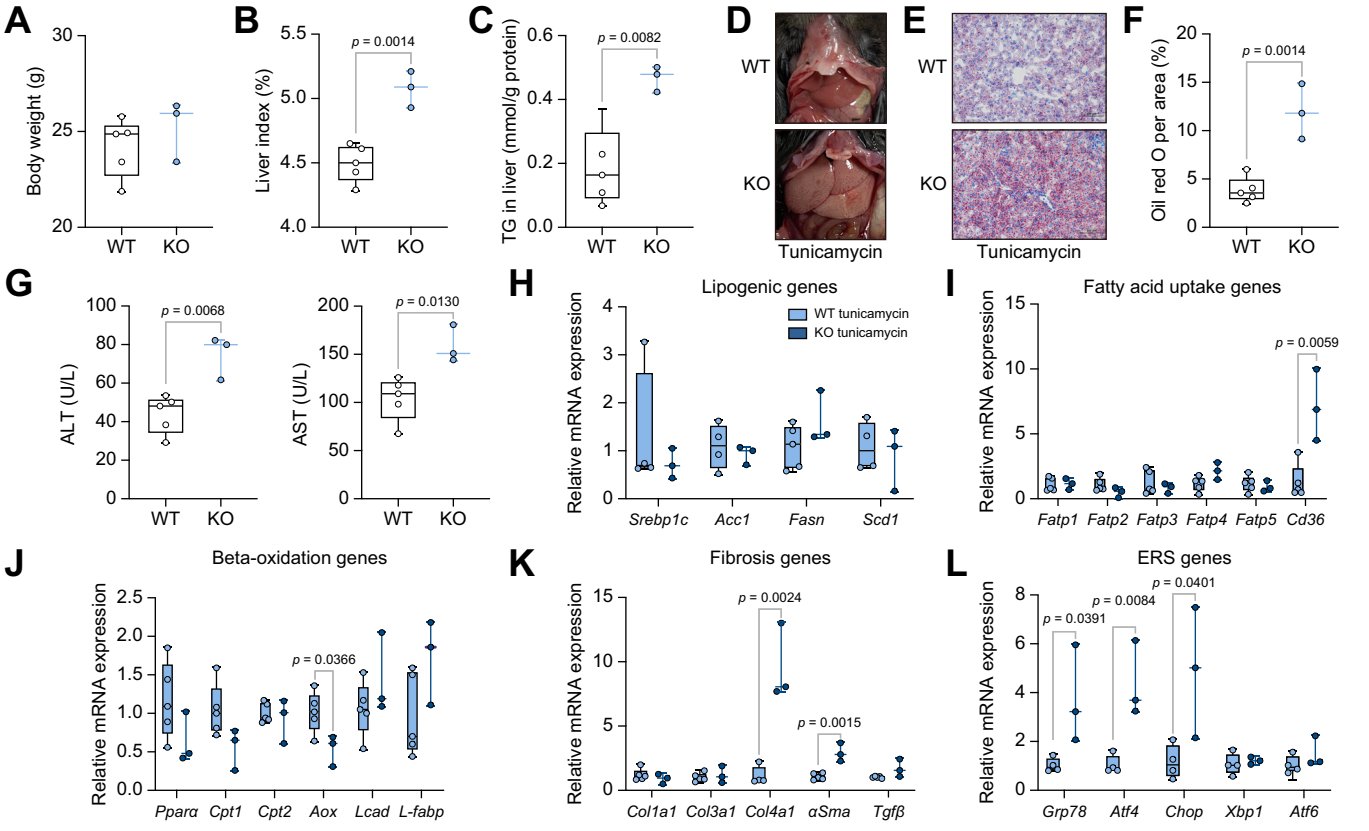

Fig. 2. *Emc10* KO mice exhibited exacerbated hepatosteatosis invoked by tunicamycin. WT (n = 5) and *Emc10* KO (n = 3) male mice were intraperitoneally injected with tunicamycin for 24 hours. (A) Body weights. (B) Liver index. (C) Liver triglyceride content. (D) Representative livers were visualized *in situ*. (E) Representative images of Oil red O staining of liver sections. Scale bars, 100 μm. (F) Liver Oil red O staining area. (G) Serum levels of ALT and AST. (H-L) Relative hepatic expression of genes as indicated, linked to lipogenesis (H), fatty acid uptake (I), beta oxidation (J), fibrosis (K), and ER stress (L). All data are presented as mean ± SEM. Statistical analyses were performed using Student's *t* test. ALT, alanine aminotransferase; AST, aspartate aminotransferase; ERS, endoplasmic reticulum stress; KO, knockout; TG, triglyceride; WT, wild-type. (This figure appears in color on the web.)

The two isoforms of EMC10 differ in the regulation of hepatic PERK-eIF2α signaling

We have previously revealed that the two isoforms of EMC10 function differently in the regulation of sperm motility.[15] Here we explored whether the two isoforms differently modulated hepatic PERK-eIF2α signaling. Thapsigargin markedly activated eIF2α signaling in HepG2 cells (Fig. S5), which was significantly blunted by overexpression of mEMC10 (Fig. 4A,B). Coincidently, overexpression of mEMC10 significantly decreased lipid accumulation in HepG2 cells challenged with thapsigargin (Fig. S6A). Given thapsigargin is not a potent inducer of lipid accumulation, palmitic acid, in combination with oleic acid, was used to invoke more hepatocytic steatosis.[26] Overexpression of mEMC10 also resulted in a significant reduction in cellular lipid accumulation under the stimulation of the lipid mixture (Fig. S6B). Taken together, these data suggest that mEMC10 has a suppressive role in hepatocytic ER stress and steatosis.

We next examined the impact of the secreted isoform in the regulation of hepatic PERK-eIF2α signaling. In HepG2 cells, recombinant scEMC10 significantly heightened PERK-eIF2α signaling activity compared with vehicle (Fig. 4C,D). In mouse livers, exogenous recombinant scEMC10 also significantly enhanced PERK-eIF2α signaling (Fig. 4E). These data indicate that the scEMC10, contrary to mEMC10, promotes hepatic UPR activation. When the activation of PERK was restrained by either a chemical inhibitor GSK2606414 or a small-interfering RNA, the heightened eIF2α phosphorylation induced by scEMC10 was totally impaired (Fig. 4F,G), suggesting scEMC10-elicited eIF2α activation is dependent on PERK.

To further explore the molecular mechanism of EMC10-regulated eIF2α activity, we determined whether the other three well-known kinases upstream of eIF2α including PKR, GCN2, and HRI, were involved in the EMC10-regulated eIF2α phosphorylation.[27] We observed under the stimulation of recombinant scEMC10 protein, HepG2 cells exhibited elevated eIF2α phosphorylation, but unchanged phosphorylation of either PKR or GCN2, and total HRI (Fig. S7A, B). We also identified that neither phosphorylation of PKR and GCN2 nor total HRI was changed in livers of either chow diet-fed *Emc10* KO, HFD-fed scEMC10-overexpressing, or tunicamycin-treated mEMC10-overexpressing mice, compared with their corresponding control mice (Fig. S7C–E). These observations suggest EMC10-modulated hepatic eIF2α signaling is exclusively dependent on PERK.

The secreted isoform of EMC10 promotes the development of hepatosteatosis in mice

We presented evidence *Emc10* KO mice lacked the two isoforms at both the mRNA and protein levels (Fig. 3).[17] To distinguish their *in vivo* roles in hepatosteatosis, we firstly

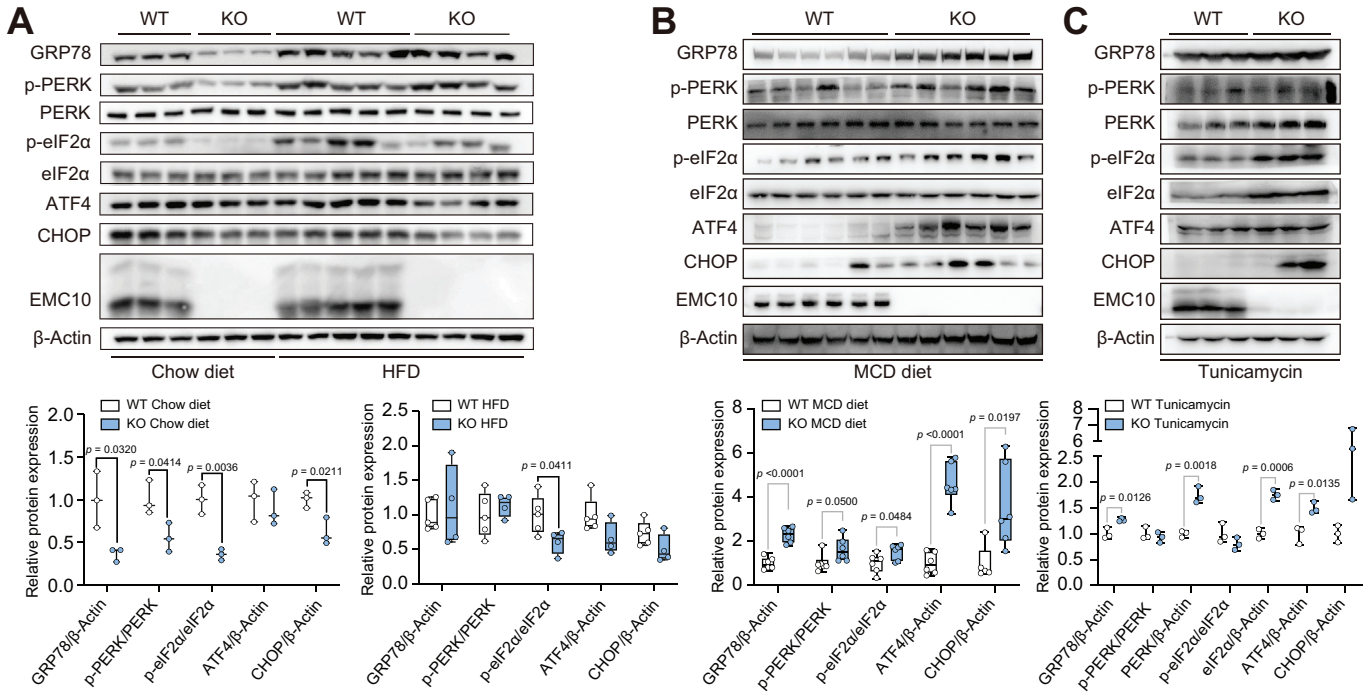

Fig. 3. EMC10 regulates hepatic PERK-eIF2α signaling in *Emc10* KO mouse models. (A-C) Hepatic levels of proteins as indicated in *Emc10* KO or WT mice fed with either chow diet (A, left), HFD (12 weeks) (A, right), MCD diet (3 weeks) (B), or tunicamycin (24 hours) (C). Quantitative analysis of these western blotting results based on densitometry were listed below. All data are presented as mean ± SEM. Statistical analyses were performed using Student's *t* test. HFD, high-fat diet; KO, knockout; MCD, methionine- and choline-deficient; WT, wild-type.

overexpressed scEMC10 in mouse using an AAV8-mediated delivery system.[17] scEMC10 overexpression resulted in a robust increase of *scEmc10* mRNA, while *mEmc10* mRNA in mouse livers was unchanged (Fig. 5A,B). Phenotypic analysis demonstrated that overexpression of scEMC10 exacerbated hepatoteatosis in wild-type mice fed a HFD, as supported by greater levels of liver index, LFC, NAS, and serum ALT compared with controls (Fig. 5C–H), concordant with greater hepatic expression of genes involved in lipogenesis, FA uptake, inflammation, fibrosis, and ER stress as well as reduced beta-oxidation gene expression in the mice overexpressing scEMC10 (Fig. 5I–N). Immunoblot analysis indicated enhanced eIF2α signaling in scEMC10-overexpressing livers (Fig. 5O,P). Similar to the findings in wild-type mice, overexpression of scEMC10 exacerbated hepatosteatosis in *Emc10* KO mice fed either a HFD or a MCD diet (Figs S8 and S9).

Taken together, these observations indicate scEMC10 promotes the development of hepatosteatosis in mouse.

The membrane-bound isoform of EMC10 ameliorates hepatosteatosis induced by tunicamycin in mouse

To explore the hepatic role of EMC10 in the context of MASLD, it is preferable to use liver-specific EMC10 mouse models. Although AAV8 is a hepatotropic virus, as a circulating factor, scEMC10 overexpressed in the liver will target other tissues, which raises a possibility that scEMC10-modulated hepatosteatosis is indirect and liver independent. To this end, we overexpressed mEMC10 specifically in the livers of mice using the hepatotropic AAV8. mEMC10 overexpression significantly increased hepatic *mEmc10* gene expression but did not affect *scEmc10* gene expression (Fig. 6A,B). There was no significant difference in either body weight or liver index between scEMC10-overexpressing and control mice (Fig. 6C,D). Of note, hepatic overexpression of mEMC10 significantly ameliorated tunicamycin-induced mouse hepatosteatosis, evidenced by significant lower levels of LFC and serum ALT and AST compared with control (Fig. 6E–I). Gene expression analysis identified increased lipogenesis, unchanged FA uptake, enhanced beta oxidation, and decreased fibrosis and ER stress in mEMC10-overexpressing livers compared to control ones (Fig. 6J–N), with the latter three – but not lipogenesis – supporting the observed steatotic phenotype. Protein analysis indicated a significantly suppressive impact of mEMC10 on hepatic ER stress (Fig. 6O).

Collectively, these data suggest mEMC10 exerts a direct role in hepatocytes decreasing ER stress and ATF4 activation in hepatosteatosis.

Neutralization of circulating scEMC10 ameliorates hepatosteatosis in mice fed a MCD diet

We have shown that a scEMC10-neutralizing antibody, termed 4C2, dramatically reduced hepatic lipid accumulation and serum ALT levels in HFD-fed mice.[17] The effect of 4C2 antibody (Ab) on hepatosteatosis was further validated in MCD diet-fed mice. 4C2 Ab did not alter body weight, but resulted in a significantly smaller liver index, as compared to control IgG (Fig. 7A, B). 4C2 Ab significantly decreased LFC and tended to lower NAS (Fig. 7C–F). qPCR analysis revealed hepatic levels of lipogenesis, FA uptake, inflammation, and ER stress were all significantly reduced, whereas beta oxidation remained unchanged and *αSma* mRNA was unexpectedly increased, in 4C2 Ab-treated mice compared with control animals (Fig. 7G–L). It

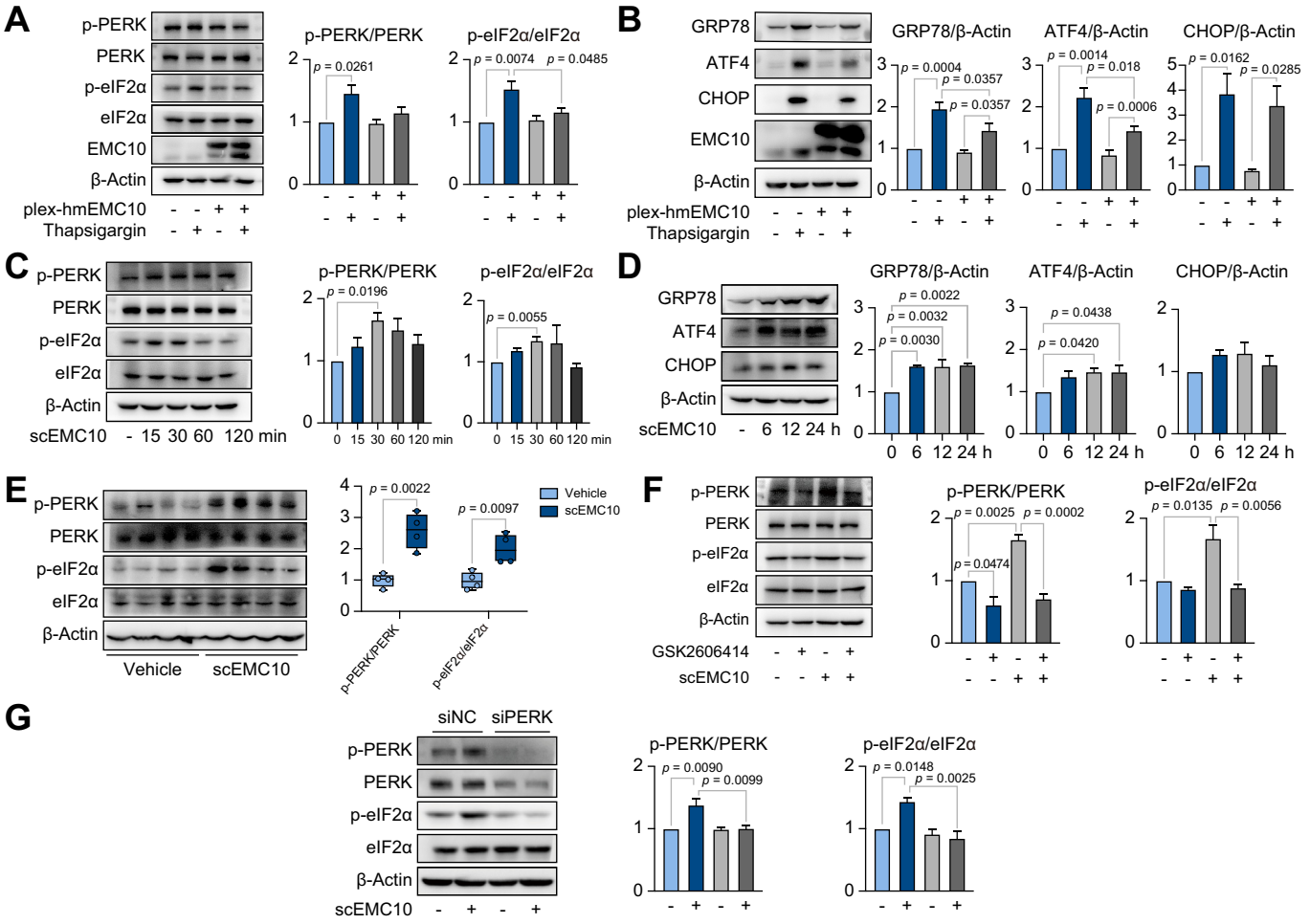

Fig. 4. Different roles of mEMC10 and scEMC10 in the regulation of hepatic PERK-eIF2α signaling. The activity of PERK-eIF2α signaling in human mEMC10-overexpressed (pLEX-hmEMC10) HepG2 cells either 15 minutes (A) or 12 hours (B) post 0.2 μM thapsigargin treatment, HepG2 cells treated with 1 μg/ml recombinant scEMC10 for various time (C,D), livers of C57BL/6J male mice intraperitoneally injected with vehicle PBS or recombinant scEMC10 (6 mg per kg body weight) for 30 minutes (E), or HepG2 cells treated with recombinant scEMC10 in combination with PERK inhibitor GSK2606414 (F) or siRNA (G). Quantitative analysis of western blotting data based on densitometry are shown on the right in each panel. All cell culture experiments were repeated 3-4 times. All data are presented as mean ± SEM. Statistical analyses were performed using Student's *t* test. hmEMC10, human membrane-bound isoform of EMC10; scEMC10, secreted isoform of EMC10; siNC, non-target control siRNA; siPERK, PERK siRNA.

has been shown that phosphorylated eIF2α and CHOP were increased in livers of MCD diet-fed mice.[23] We observed 4C2 Ab significantly decreased hepatic eIF2α phosphorylation and CHOP compared with control IgG (Fig. 7M). Short-term 4C2 Ab treatment, compared with control IgG, did not alter the steatotic phenotype in MCD diet-fed mice (Fig. S10A–F), but significantly changed hepatic expression of most of the examined genes, especially genes involved in ER stress with dramatic reductions in expression (Fig. S10G–L), and significantly suppressed hepatic eIF2α phosphorylation and CHOP (Fig. S10M). The change in UPR activity prior to the change in steatosis suggests suppression of the UPR as a cause for 4C2 Ab-mitigated hepatosteatosis, rather than a consequence.

Collectively, these findings suggest inhibition of scEMC10 as a promising therapeutic target for MASLD.

Serum scEMC10 positively, while hepatic mEMC10 negatively, correlated with MASLD in humans

To explore the role of scEMC10 and mEMC10 in human MASLD, serum scEMC10 levels, LFC and hepatic mRNA levels of *scEMC10*, *mEMC10*, and PERK-eIF2α signaling downstream targets (including *ATF4*, *CHOP*, and *CD36*) were measured in a Caucasian cohort of participants with MASLD *vs.* non-MASLD controls (Table S1). We observed serum scEMC10 levels were significantly elevated in MASLD participants with the changes of LFC, NAS, and fibrosis score (Fig. 8A–C). Hepatic *mEMC10* transcript levels were significantly reduced in participants with MASLD compared with non-MASLD controls, but exhibited no difference in MASLD participants with different stratifications of either LFC, NAS, or fibrosis score (Fig. 8D–F). Correlative analysis indicated serum scEMC10 levels were positively associated with LFC, hepatic mRNA levels of *scEMC10*, *ATF4*, and *CHOP* as well as serum ALT, AST, and GGT, while being negatively associated with hepatic *mEMC10* transcript (Fig. 8G), and hepatic *mEMC10* mRNA levels were negatively associated with LFC, and serum scEMC10, ALT, AST, and GGT (Fig. 8G).

Regarding downstream targets of PERK-eIF2α signaling, we observed higher levels of hepatic *CHOP* transcript were significantly associated with higher levels of LFC, NAS, and fibrosis (Fig. S11A–C). Hepatic *ATF4* transcript levels were

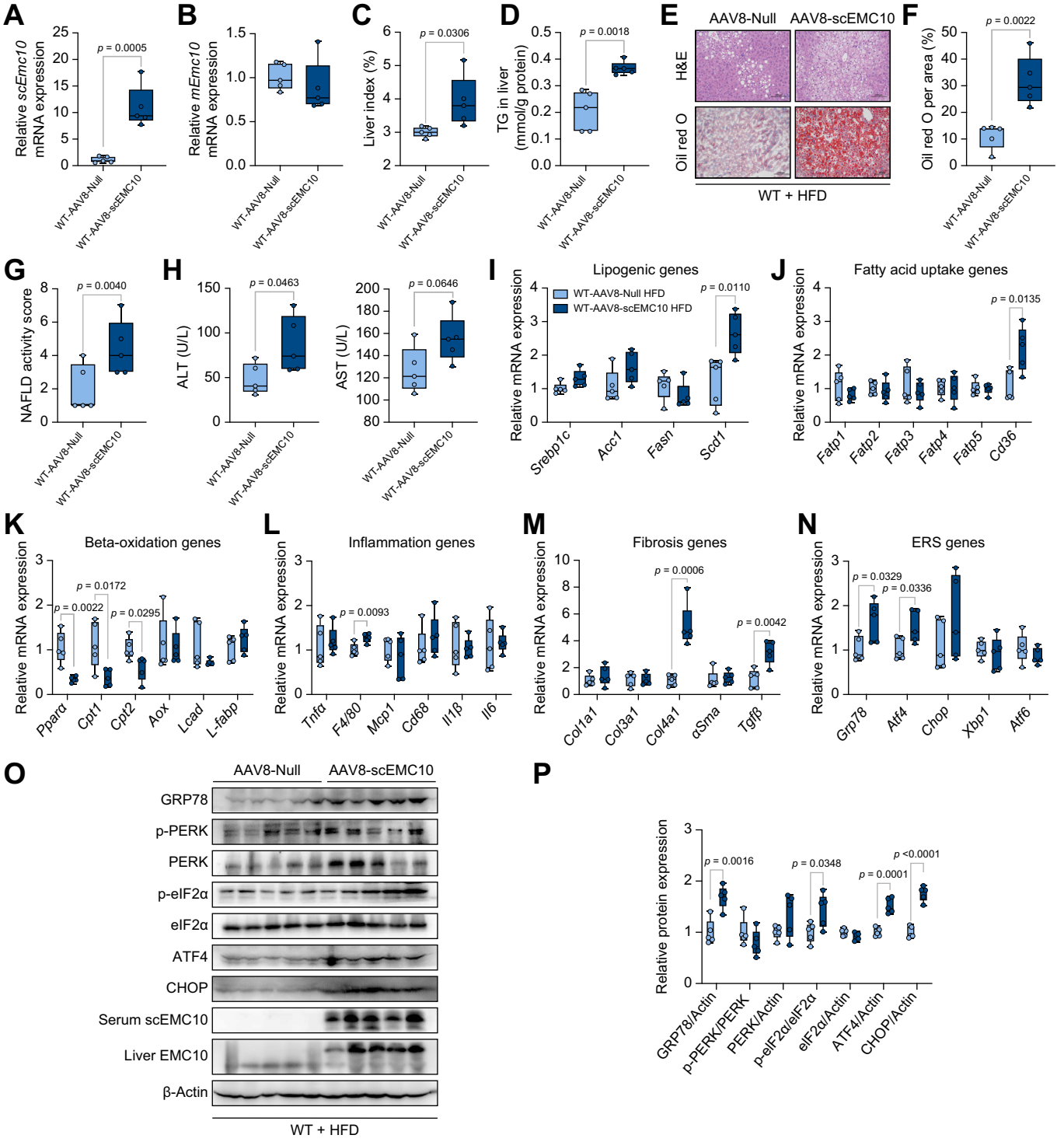

Fig. 5. scEMC10 overexpression promotes hepatosteatosis in wild-type mice fed a HFD. AAV8-encoding human scEMC10 (AAV8-scEMC10) or control virus (AAV8-null) were administrated to male C57BL/6J WT mice via tail vein injection. Five weeks post AAV8 injection, these mice were fed a HFD for 20 weeks. (A-B) Hepatic mRNA levels of *scEmc10* (A) and *mEmc10* (B). (C) Liver index. (D) Liver triglyceride content. (E) Representative images of H&E and Oil red O staining of liver sections. Scale bars, 100 μm. (F) Liver Oil red O staining area. (G) NAFLD activity score. (H) Serum levels of ALT and AST. (I–N) Relative hepatic expression of genes as indicated, linked to lipogenesis (I), fatty acid uptake (J), beta oxidation (K), inflammation (L), fibrosis (M), and ER stress (N). (O–P) Hepatic PERK-eIF2α signaling was determined using western blotting and its associated quantitative analysis. n = 5 for each animal group. All data are presented as mean ± SEM. Statistical analyses were performed using Student's *t* test. AAV8, adeno-associated virus 8; ALT, alanine aminotransferase; AST, aspartate aminotransferase; ERS, endoplasmic reticulum stress; HFD, high-fat diet; mEMC10, membrane-bound isoform of EMC10; scEMC10, secreted isoform of EMC10; TG, triglyceride; WT, wild-type. (This figure appears in color on the web.)

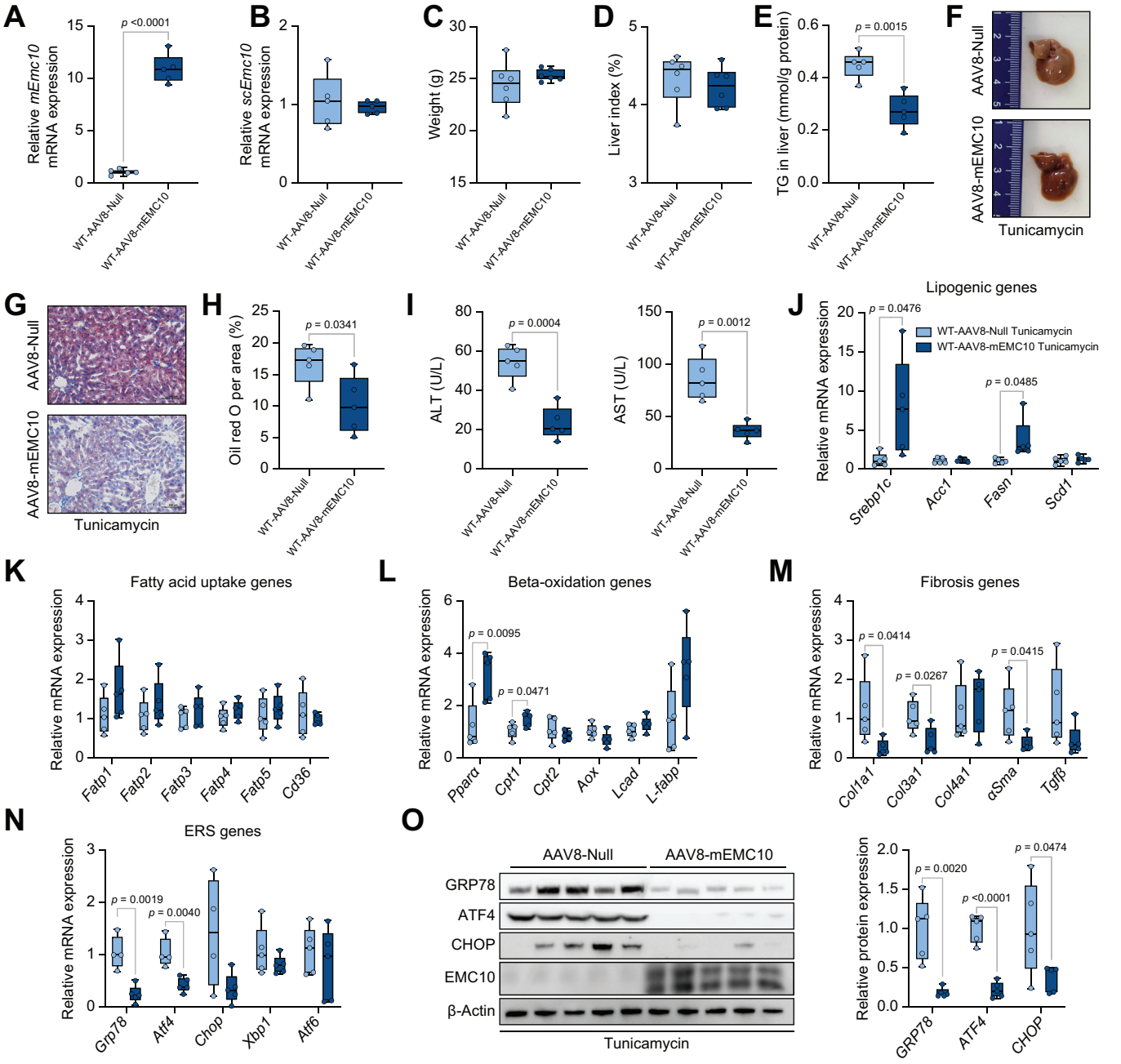

Fig. 6. Hepatic overexpression of mEMC10 ameliorated tunicamycin-induced hepatosteatosis in mouse. AAV8-encoding mouse mEMC10 (AAV8-mEMC10) or control virus (AAV8-null) were administrated to male C57BL/6J WT mice via tail vein injection. Six weeks post AAV8 injection, these mice were intraperitoneally injected with tunicamycin for 48 hours. (A-B) Hepatic mRNA levels of *mEmc10* (A) and *scEmc10* (B). (C) Body weights. (D) Liver index. (E) Liver triglyceride content. (F) Representative livers were visualized *in situ*. (G) Representative images of Oil red O staining of liver sections. Scale bars, 100 μm. (H) Liver Oil red O staining area. (I) Serum levels of ALT and AST. (J-N), Relative hepatic expression of genes as indicated, linked to lipogenesis (J), fatty acid uptake (K), beta oxidation (L), fibrosis (M), and ER stress (N). (O) Hepatic GRP78, ATF4, and CHOP were determined using western blotting. Quantitative analysis of western blotting results (left) based on densitometry were shown right. n = 5 for each animal group. All data are presented as mean ± SEM. Statistical analyses were performed using Student's *t* test. AAV8, adeno-associated virus 8; ALT, alanine aminotransferase; AST, aspartate aminotransferase; ERS, endoplasmic reticulum stress; mEMC10, membrane-bound isoform of EMC10; scEMC10, secreted isoform of EMC10; TG, triglyceride; WT, wild-type. (This figure appears in color on the web.)

significantly higher in participants with LFC of >25% and with NAS of ≥5 than controls (Fig. S11D–F). Both hepatic *scEMC10* and *CD36* transcripts remained unchanged in the Caucasian cohort regardless of being stratified by either LFC, NAS, or fibrosis score (Fig. S11G–L).

Concordant with reduced expression in livers of participants with MASLD, there was a striking reduction in *mEmc10* gene expression in HFD-fed mouse livers and a slight reduction in tunicamycin-treated mouse livers (Fig. S12).

In another cohort of Chinese participants with MASLD who underwent GLP-1RA treatment (Table S2), GLP-1RAs significantly reduced both LFC and serum scEMC10 by 27.4% and 31.3%, respectively, at 3 months (Fig. 8H, I). The reduction of LFC was positively associated with the change of serum scEMC10 (Fig. 8J).

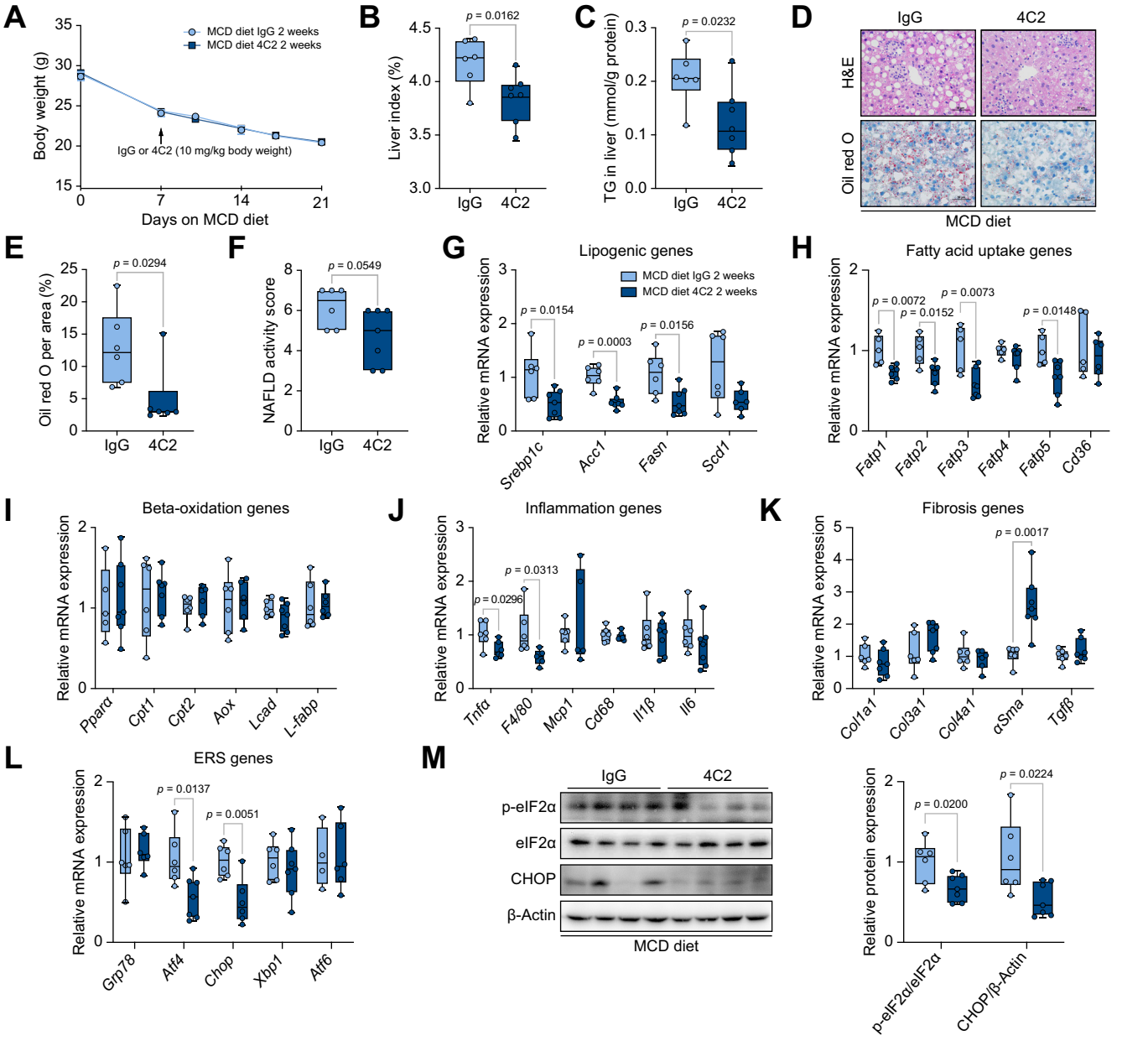

Fig. 7. scEMC10 neutralization ameliorates hepatosteatosis in mice fed a MCD diet. C57BL/6J male mice were fed with a MCD diet for 1 week prior to intraperitoneal injection with scEMC10-neutralizing antibody (4C2) (10 mg per kg body weight) or equivalent control IgG for 2 weeks, twice a week. (A) Body weights. (B) Liver index. (C) Liver triglyceride content. (D) Representative images of H&E and Oil red O staining of liver sections. Scale bars, 50 μm. (E) Liver Oil red O staining area. (F) NAFLD activity score. (G-L) Relative hepatic expression of genes as indicated, linked to lipogenesis (G), fatty acid uptake (H), beta oxidation (I), inflammation (J), fibrosis (K), and ER stress (L). (M) Hepatic eIF2α signaling was determined using western blotting. Quantitative analysis of western blotting results (left) based on densitometry were shown right. n = 6-7 for each animal group. All data are presented as mean ± SEM. Statistical analyses were performed using Student's *t* test. 4C2, scEMC10-neutralizing antibody; ERS, endoplasmic reticulum stress; MCD, methionine- and choline-deficient; TG, triglyceride. (This figure appears in color on the web.)

Collectively, these clinical data indicate scEMC10 positively, while hepatic mEMC10 negatively, correlates with MASLD, as well as implying that mEMC10 exerts a direct role in suppressing MASLD.

Discussion

The findings of this study suggest the two isoforms of EMC10 play different roles in MASLD. The inverse association of hepatic mEMC10 with human MASLD, in combination with its suppressive impacts on hepatic ER stress and steatosis in both cell culture and mouse models, highlight a direct role of mEMC10 in MASLD via decreasing hepatic ER stress and ATF4 activation. Meanwhile, scEMC10 has been positively associated with obesity and insulin resistance in both humans and mice,[17,18] which are sufficient to induce MASLD.[19] Given HFD-fed *Emc10* KO or scEMC10-overexpressing mice exhibit changes in body fat mass and insulin sensitivity, it is most likely that scEMC10 largely exerts an indirect role in MASLD via modulation of the systemic fat load to liver, rather than directly acting on hepatocytes. The observation that overexpression of scEMC10 exacerbated, while antibody neutralization of circulating scEMC10 ameliorated,

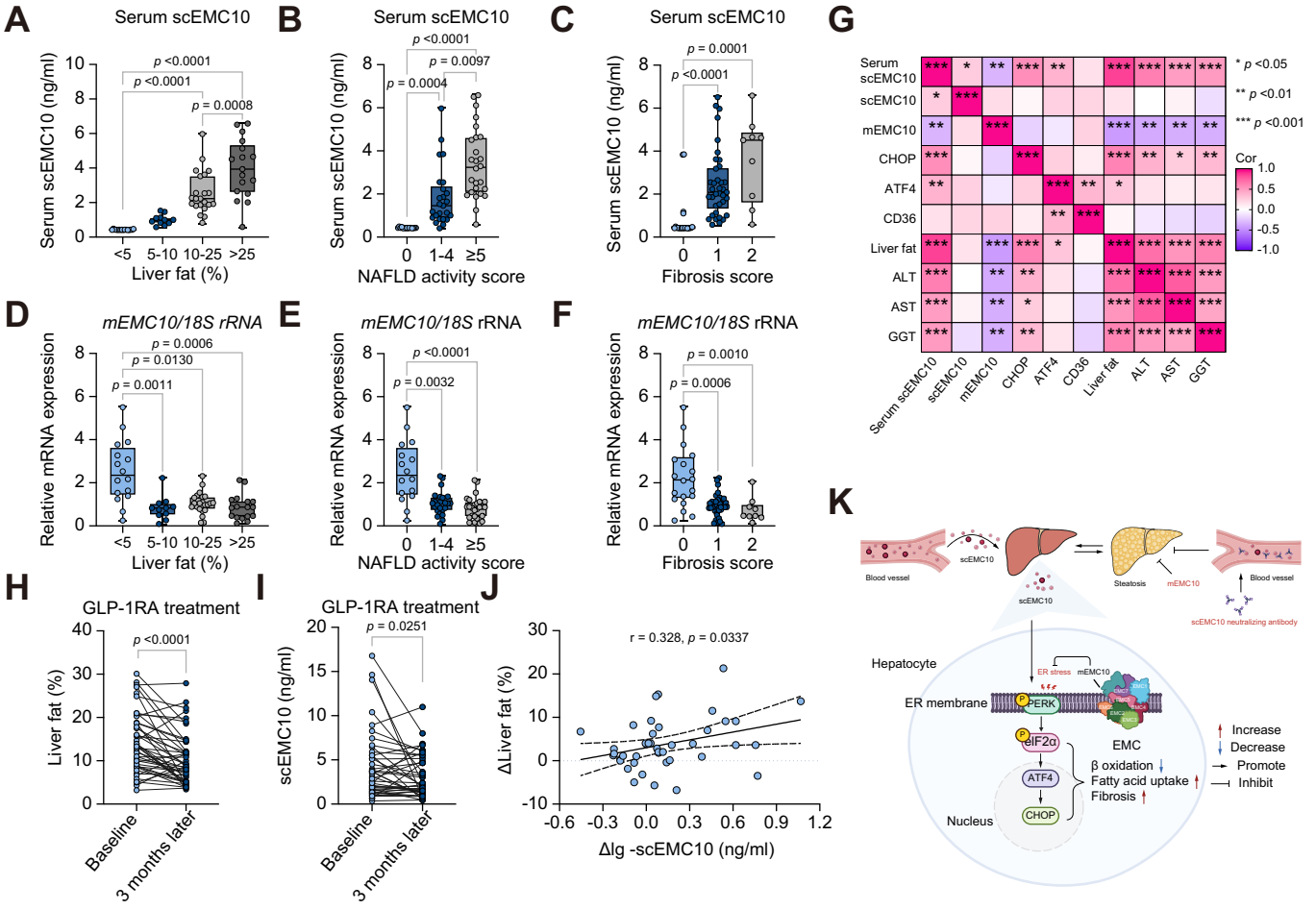

Fig. 8. The association of EMC10 with human MASLD. Levels of serum scEMC10 (A-C) and hepatic *mEMC10* transcript (D-F) in participants with varying LFC (<5%, n = 16; 5%-10%, n = 11; 10%-25%, n = 22; >25%, n = 17) (A, D), different NAFLD activity score (0, n = 15; 1-4, n = 25; ≥5, n = 26) (B, E), and different fibrosis score (0, n = 20; 1, n = 37; 2, n = 9) (C, F) from a Caucasian cohort. (G) Correlations among EMC10 and other associated parameters in the Caucasian cohort. (H & I) LFC (H) and serum scEMC10 concentration (I) before and 3 months after GLP-1RA treatment (n = 45). (J) Correlation between the change of serum scEMC10 concentration and the change of LFC after GLP-1RA treatment. (K) A schematic diagram depicting the roles of the two isoforms of EMC10 in the pathogenesis of hepatosteatosis. All data are presented as mean ± SEM or median with interquartile range. Statistical analyses were performed using Student's *t* test, Pearson correlation's test, or Wilcoxon signed-rank test. GLP-1RA, GLP-1 receptor agonist; LFC, liver fat content; MASLD, metabolic dysfunction-associated steatotic liver disease; mEMC10, membrane-bound isoform of EMC10; scEMC10, secreted isoform of EMC10. (This figure appears in color on the web.)

hepatosteatosis in MCD diet mouse models, together with *in vitro* data showing recombinant scEMC10 protein activated PERK-eIF2α-ATF4 signaling, also suggest scEMC10 directly contributes to MASLD via activation of hepatic ER stress.

The UPR cannot be simply defined as an adaptive mechanism to cope with misfolded proteins, and thereby exert cytoprotective effects. It has been implicated in the regulation of hepatic lipid homeostasis through various metabolic pathways, including lipogenesis, FA uptake, and beta oxidation.[2] The transcriptional factor ATF4 is translationally upregulated upon phosphorylation of eIF2α and activates the expression of multiple genes involved in hepatic lipid metabolism.[8,28] CD36, which is a key player in FA uptake and strikingly regulated by EMC10, has been shown to be upregulated by ATF4 in the context of palmitate or tunicamycin treatment, which in turn led to heightened intracellular triacylglycerol accumulation and cell death in hepatocytes.[28] It has been reported that ATF4 positively regulates hepatic expression of lipogenic genes, but did not regulate beta-oxidation genes.[8] In this work, we observed that expression of genes involved in either beta oxidation or FA uptake was consistent with both hepatic PERK-eIF2α-ATF4 signaling and steatosis, while lipogenic genes were not, suggesting modulation of both hepatic beta oxidation and FA uptake, rather than *de novo* lipogenesis, as a causative mechanism underlying EMC10-impacted hepatosteatosis.

The reduction of serum scEMC10 accompanied by the decrease of LFC evoked by GLP-1RAs in humans with MASLD and the mitigation of mouse hepatosteatosis by scEMC10 neutralization, indicate that scEMC10 is a promising therapeutic target for the treatment of MASLD. Given that mEMC10 is localized in the ER lumen,[14] targeting scEMC10 via either a neutralizing antibody or a receptor antagonist will avoid inhibiting mEMC10, which is required for the maintenance of male fertility, neuronal development, and hepatic UPR homeostasis,[15,16,29–31] thus avoiding unfavorable effects.

Our discovery of a regulatory action of mEMC10 on UPR homeostasis may inform the pathogenesis of a newly identified neurodevelopmental disorder caused by mEMC10 disruption, including intellectual disability, language impairment, variable seizures and dysmorphic features.[29–31] The disruption arises

from *EMC10* gene variants, which destroy the C-terminal transmembrane domain of mEMC10 or result in a truncation abolishing the C-terminal region.[29–31] PERK-eIF2α signaling has been implicated in neurodegenerative diseases. Severe or chronic ER stress leads to sustained phosphorylation of eIF2α, in turn repressing the synthesis of synaptic proteins, eventually eliciting a proapoptotic program of neurons.[32] Antagonists of PERK-eIF2α signaling have been reported to reduce neurodegeneration and exert neuroprotective effects.[33] In this scenario, reconstitution of mEMC10 via gene therapy or administration of antagonists of PERK-eIF2α signaling could be promising therapeutics for neurodevelopmental disorders in patients carrying *EMC10* gene variants.

There are limitations in this study. The two isoforms of EMC10 are transcribed from one single gene in both mice and humans.[15] We observed the regulation on gene expression of the two isoforms was distinct in steatotic livers, suggesting a post-transcriptional mechanism underlying the regulation of the two isoforms. The underlying mechanism, however, remains unidentified. The observation, in mouse models, that overexpression of one isoform did not alter expression of the other one excludes the possibility that one isoform can be transformed to the other. Currently we do not have antibodies to specifically recognize the two isoforms individually in the liver or an ELISA kit to detect scEMC10 in mouse serum, meaning the exact protein levels of the two isoforms are unknown. Furthermore, whether and how much the hepatoprotective effects of scEMC10 ablation are dependent on the changes of body fat mass and insulin sensitivity need to be clarified by suppressing the increases in thermogenesis in brown adipose tissue of *Emc10* KO mice and then testing the effects on steatosis.

As summarized in Fig. 8K, we present evidence that scEMC10 promotes, while mEMC10 suppresses, the activation of hepatocytic PERK-eIF2α-ATF4 signaling and associated hepatosteatosis in mice. These results are further supported by clinical findings that serum scEMC10 positively, while hepatic mEMC10 inversely, correlates with MASLD in humans. This work distinguishes the roles of the two isoforms of EMC10 in MASLD and identifies scEMC10 as a promising therapeutic target for MASLD.

Affiliations

[1]*Department of Endocrinology, Huashan Hospital, Shanghai Medical College, Fudan University, Shanghai, China;* [2]*Helmholtz Institute for Metabolic, Obesity and Vascular Research (HI-MAG) of the Helmholtz Zentrum München at the University of Leipzig and University Hospital Leipzig, Leipzig, Germany;* [3]*Medical Department III – Endocrinology, Nephrology, Rheumatology, University of Leipzig Medical Center, Leipzig, Germany;* [4]*Department of Endocrinology and Metabolism, The Affiliated Hospital of Qingdao University, Qingdao, China;* [5]*Department of Physiology & Biophysics, University of Illinois at Chicago, Chicago, IL, USA;* [6]*Department of Visceral, Transplant, Thoracic and Vascular Surgery, University Hospital Leipzig, Leipzig, Germany;* [7]*Department of Endocrinology, The Second Affiliated Hospital, School of Medicine, Zhejiang University, Hangzhou, China*

Abbreviations

Ab, antibody; AAV, adeno-associated virus; ALT, alanine aminotransferase; AST, aspartate aminotransferase; ATF4, activating transcription factor 4; ATF6, activating transcription factor 6; CHOP, C/EBP homologous protein; EMC, endoplasmic reticulum membrane protein complex; EMC10, endoplasmic reticulum membrane protein complex subunit 10; ER, endoplasmic reticulum; eIF2α, eukaryotic translation initiation factor 2α; FA, fatty acid; GCN2 (EIF2AK4), eukaryotic translation initiation factor 2 alpha kinase 4; GGT, gamma-glutamyltransferase; GLP-1RA, GLP-1 receptor agonist; GRP78, glucose-regulated protein 78; HFD, high-fat diet; HRI (EIF2AK1), eukaryotic translation initiation factor 2 alpha kinase 1; IRE1α, inositol-requiring enzyme 1α; ISR, integrated stress response; KO, knockout; LFC, liver fat content; MASLD, metabolic dysfunction-associated steatotic liver disease; MCD, methionine- and choline-deficient; mEMC10, membrane-bound isoform of endoplasmic reticulum membrane protein complex subunit 10; NAS, NAFLD activity score; PERK, protein kinase RNA-like endoplasmic reticulum kinase; PKR (EIF2AK2), eukaryotic translation initiation factor 2 alpha kinase 2; scEMC10, secreted isoform of endoplasmic reticulum membrane protein complex subunit 10; SNP, single-nucleotide polymorphism; UPR, unfolded protein response; WT, wild-type; XBP1, X-box binding protein 1.

Financial support

The work was supported by National Natural Science Foundation of China (No. 81873645) and Science and Technology Commission of Shanghai Municipality (No. 22140902700) to X. W., and Shandong Provincial Health Commission (No. S190009280000) to Y. W.

Conflict of interest

M.B. received honoraria as a consultant and speaker from Amgen, AstraZeneca, Bayer, Boehringer-Ingelheim, Lilly, Novo Nordisk, Novartis, Pfizer and Sanofi.

Please refer to the accompanying ICMJE disclosure forms for further details.

Authors' contributions

K. C., Y. W. & J. Y. wrote the manuscript, experimental design & work; N. K. transcriptional analysis of human liver samples & determination of serum scEMC10 in the Caucasian cohort; C.L. clinical work & determination of serum scEMC10 in the Chinese cohort; J. D. statistical analysis of the data; S. J. cell culture experiments; L. C. animal work & qPCR analysis; S. L. establishment of mouse models; Y. L. blood samples & clinical work on the Chinese cohort; Y. Y. clinical work on the Chinese cohort; X. L. experimental work, histological analysis of mouse tissue; Q. M. mouse experimental work *in vivo* with antibody intervention; C. W. L. conceptual input & discussion on the data; Y. W. supervised the study on the Chinese cohort; A. D. surgical expertise & provision of human liver biopsy samples; M. B. supervised the study on the Caucasian cohort; X. W. wrote the paper, conceived the project & supervised the study.

Data availability statement

The data supporting the findings from this study are available within the manuscript and its supplementary information. Further information and requests for resources and reagents should be directed to and will be fulfilled by the Corresponding Author, Prof. X. Wang.

Acknowledgements

We thank Samuel M. Lockhart for his help in discussing the data and preparing the manuscript. We also thank Dr. Junli Liu for providing HepG2 cells and Dr. Daming Gao for providing pMD·2G and psPAX2 plasmids as well as 293T cells. The graphical abstract and the schematic diagram in Fig. 8K were created with BioRender.com.

Supplementary data

Supplementary data to this article can be found online at https://doi.org/10.1016/j.jhep.2024.03.047.

References

Author names in bold designate shared co-first authorship

[1] Hotamisligil GS. Endoplasmic reticulum stress and the inflammatory basis of metabolic disease. Cell 2010;140:900–917.

[2] Lebeaupin C, Vallee D, Hazari Y, et al. Endoplasmic reticulum stress signalling and the pathogenesis of non-alcoholic fatty liver disease. J Hepatol 2018;69:927–947.

[3] Puri P, Mirshahi F, Cheung O, et al. Activation and dysregulation of the unfolded protein response in nonalcoholic fatty liver disease. Gastroenterology 2008;134:568–576.

[4] **Gregor MF**, **Yang L**, Fabbrini E, et al. Endoplasmic reticulum stress is reduced in tissues of obese subjects after weight loss. Diabetes 2009;58:693–700.
[5] **Ozcan U**, **Cao Q**, Yilmaz E, et al. Endoplasmic reticulum stress links obesity, insulin action, and type 2 diabetes. Science 2004;306:457–461.
[6] Henkel AS, Dewey AM, Anderson KA, et al. Reducing endoplasmic reticulum stress does not improve steatohepatitis in mice fed a methionine- and choline-deficient diet. Am J Physiol Gastrointest Liver Physiol 2012;303:G54–G59.
[7] Oyadomari S, Harding HP, Zhang Y, et al. Dephosphorylation of translation initiation factor 2alpha enhances glucose tolerance and attenuates hepatosteatosis in mice. Cell Metab 2008;7:520–532.
[8] **Xiao G**, **Zhang T**, Yu S, et al. ATF4 protein deficiency protects against high fructose-induced hypertriglyceridemia in mice. J Biol Chem 2013;288:25350–25361.
[9] Seo J, Fortuno 3rd ES, Suh JM, et al. Atf4 regulates obesity, glucose homeostasis, and energy expenditure. Diabetes 2009;58:2565–2573.
[10] Yeh KY, Lai CY, Lin CY, et al. ATF4 overexpression induces early onset of hyperlipidaemia and hepatic steatosis and enhances adipogenesis in zebrafish. Sci Rep 2017;7:16362.
[11] Satoh T, Ohba A, Liu Z, et al. dPob/EMC is essential for biosynthesis of rhodopsin and other multi-pass membrane proteins in Drosophila photoreceptors. Elife 2015;4:e06306.
[12] Jonikas MC, Collins SR, Denic V, et al. Comprehensive characterization of genes required for protein folding in the endoplasmic reticulum. Science 2009;323:1693–1697.
[13] Richard M, Boulin T, Robert VJ, et al. Biosynthesis of ionotropic acetylcholine receptors requires the evolutionarily conserved ER membrane complex. Proc Natl Acad Sci U S A 2013;110:E1055–E1063.
[14] Bai L, You Q, Feng X, et al. Structure of the ER membrane complex, a transmembrane-domain insertase. Nature 2020;584:475–478.
[15] Liu L, Mao S, Chen K, et al. Membrane-bound EMC10 is required for sperm motility via maintaining the homeostasis of cytoplasm sodium in sperm. Int J Mol Sci 2022;23:10069.
[16] Zhou Y, Wu F, Zhang M, et al. EMC10 governs male fertility via maintaining sperm ion balance. J Mol Cell Biol 2018;10:503–514.
[17] **Wang X**, **Li Y**, **Qiang G**, et al. Secreted EMC10 is upregulated in human obesity and its neutralizing antibody prevents diet-induced obesity in mice. Nat Commun 2022;13:7323.
[18] **Chen K**, **Dai J**, Kloting N, et al. Serum scEMC10 levels are negatively associated with resting metabolic rate and age in humans. J Clin Endocrinol Metab 2023;108:e1074–e1081.
[19] Fabbrini E, Sullivan S, Klein S. Obesity and nonalcoholic fatty liver disease: biochemical, metabolic, and clinical implications. Hepatology 2010;51:679–689.
[20] Loomba R, Friedman SL, Shulman GI. Mechanisms and disease consequences of nonalcoholic fatty liver disease. Cell 2021;184:2537–2564.
[21] Rinella ME, Elias MS, Smolak RR, et al. Mechanisms of hepatic steatosis in mice fed a lipogenic methionine choline-deficient diet. J Lipid Res 2008;49:1068–1076.
[22] Rizki G, Arnaboldi L, Gabrielli B, et al. Mice fed a lipogenic methionine-choline-deficient diet develop hypermetabolism coincident with hepatic suppression of SCD-1. J Lipid Res 2006;47:2280–2290.
[23] Rahman SM, Schroeder-Gloeckler JM, Janssen RC, et al. CCAAT/enhancing binding protein beta deletion in mice attenuates inflammation, endoplasmic reticulum stress, and lipid accumulation in diet-induced nonalcoholic steatohepatitis. Hepatology 2007;45:1108–1117.
[24] Luo L, Jiang W, Liu H, et al. De-silencing Grb10 contributes to acute ER stress-induced steatosis in mouse liver. J Mol Endocrinol 2018;60:285–297.
[25] DeZwaan-McCabe D, Sheldon RD, Gorecki MC, et al. ER stress inhibits liver fatty acid oxidation while unmitigated stress leads to anorexia-induced lipolysis and both liver and kidney steatosis. Cell Rep 2017;19:1794–1806.
[26] Feldstein AE, Canbay A, Guicciardi ME, et al. Diet associated hepatic steatosis sensitizes to Fas mediated liver injury in mice. J Hepatol 2003;39:978–983.
[27] Ron D, Walter P. Signal integration in the endoplasmic reticulum unfolded protein response. Nat Rev Mol Cell Biol 2007;8:519–529.
[28] **Griffiths A**, **Wang J**, Song Q, et al. ATF4-mediated CD36 upregulation contributes to palmitate-induced lipotoxicity in hepatocytes. Am J Physiol Gastrointest Liver Physiol 2023;324:G341–G353.
[29] Umair M, Ballow M, Asiri A, et al. EMC10 homozygous variant identified in a family with global developmental delay, mild intellectual disability, and speech delay. Clin Genet 2020;98:555–561.
[30] Shao DD, Straussberg R, Ahmed H, et al. A recurrent, homozygous EMC10 frameshift variant is associated with a syndrome of developmental delay with variable seizures and dysmorphic features. Genet Med 2021;23:1158–1162.
[31] Kaiyrzhanov R, Rocca C, Suri M, et al. Biallelic loss of EMC10 leads to mild to severe intellectual disability. Ann Clin Transl Neurol 2022;9:1080–1089.
[32] Hetz C, Zhang K, Kaufman RJ. Mechanisms, regulation and functions of the unfolded protein response. Nat Rev Mol Cell Biol 2020;21:421–438.
[33] Marciniak SJ, Chambers JE, Ron D. Pharmacological targeting of endoplasmic reticulum stress in disease. Nat Rev Drug Discov 2022;21:115–140.